PHYSICAL REVIEW B **95**, 201303(R) (2017)

Efficiency enhancement of the coherent electron spin-flip Raman scattering through thermal phonons in (In,Ga)As/GaAs quantum dots

J. Debus,[1,*] D. Kudlacik,[1] P. Waldkirch,[1] V. F. Sapega,[2] S. Scholz,[3] A. Ludwig,[3] A. D. Wieck,[3] and M. Bayer[1,2]

[1]*Experimentelle Physik 2, Technische Universität Dortmund, 44227 Dortmund, Germany*

[2]*Ioffe Institute, Russian Academy of Sciences, 194021 St. Petersburg, Russia*

[3]*Angewandte Festkörperphysik, Ruhr-Universität Bochum, 44780 Bochum, Germany*

(Received 27 February 2017; revised manuscript received 9 April 2017; published 18 May 2017)

The spin-flip Raman scattering efficiency of the resident electron is thermally enhanced in singly charged (In,Ga)As/GaAs quantum dots, for probing the *s*- or *p*-shell trions. The Raman shift, polarization characteristics, and spectral position of the resonant scattering profile are insensitive to the sample temperature up to 50 K. This indicates a thermally robust mechanism of the coherent electron spin-flip based on exchange interaction. The background of the scattering spectra, whose intensity increases also by about one order of magnitude with temperature, is associated with acoustic phonon scattering. We propose that acoustic phonons enhance the spin-flip probability of the resident electron with growing temperature. The coherent spin-flip Raman scattering is ultimately suppressed at temperatures, which are a few times lower than that required for thermal trion dissociation.

DOI: 10.1103/PhysRevB.95.201303

Semiconductor quantum dots (QDs) are considered as an appealing material system for spin electronics and quantum technologies due to potential advantages in the availability of advanced fabrication techniques and, for instance, connectivity with other semiconductor hardware [1]. The three-dimensional confinement can moreover lead to rather long coherence times of confined charges and spins [2,3]. However, multiple interactions in the many-body environment, in particular, thermal phonons, typically cause a rapid loss of coherence. For exciton complexes in QDs, the interaction with acoustic phonons reduces the coherence even at liquid helium temperature [4,5]. For confined carrier spins, the coherence is maintained to higher temperatures; in self-assembled (In,Ga)As QDs the electron spin coherence time was found to be constant up to about 20 K, while dropping fast into the nanosecond range above it [6,7]. Therefore, also coherent manipulations have to be performed in this temperature range. Up to now, only few excitations in solid-state systems exhibit the necessary robustness to be manipulated coherently at room temperature, such as nuclear spins or carrier spins localized at deep defects [8,9].

Coherent phonons have been suggested for establishing an interaction between quantum states in nanostructures [10,11]. Whether, however, thermal phonons could contribute to manipulation within the limits set for maintaining coherence has not been explored so far. Light-matter interaction, whose probability intrinsically depends on phonons, is the principle of Raman scattering. As it can be used to flip and thereby orient spins, it provides an essential step in spin manipulation [12]. In this respect, one deals with resonant spin-flip Raman scattering (SFRS), which is a coherent photon-spin scattering process [13,14].

We observe a thermal enhancement of the SFRS efficiency for the resident electron in singly charged (In,Ga)As/GaAs QDs, where the spin flip is mediated by resonant trion excitation. The intensities of the electron-SFRS and background, which is assigned to acoustic phonon scattering, increase by about one order of magnitude with temperature rising from 6 to 28 K, for probing the *s*- or *p*-shell trions. The Raman shift, polarization characteristics, and spectral position of the resonance profile of the electron-SFRS are insensitive to the sample temperature up to 50 K; hence, the mechanism of the electron spin-flip based on exchange interaction is considered thermally robust. We propose that at elevated temperature acoustic phonons additionally induce the electron spin-flip and mediate ground-excited-state mixing thus opening spin-flip scattering channels. At high temperature they may however lead in combination with charge fluctuations of the QD environment to pure trion dephasing, which broadens the SFRS line profile and ultimately quenches the spin-flip process: The coherent SFRS process is annihilated at temperatures that are a few times lower than that required for thermal trion dissociation. The enhancement of the SFRS efficiency highlights that thermal phonons—rather astonishingly—do not destroy the coherent spin-flip scattering process, which is appealing for spin manipulation in III-V semiconductors without the need of liquid helium temperatures.

We studied two ensembles of self-assembled (In,Ga)As/GaAs QDs, fabricated by molecular-beam epitaxy on a (100)-oriented GaAs substrate and thermally annealed after growth at 920 and 945 °C, respectively. The dots were charged in average by a single electron. Both samples demonstrate similar results; in the following mainly the data, which are measured for the QDs annealed at 920 °C, will be presented. The samples were mounted strain free inside a magnet cryostat that provided magnetic fields up to 10 T. The QDs were excited by a tunable continuous-wave Ti:sapphire laser with a power density of about 0.5 W/cm^2. The QD emission was resolved by a double monochromator equipped with a Peltier-cooled GaAs photomultiplier. The backscattered SFRS experiments were performed in Voigt geometry ($\theta = 90^\circ$) and in a tilted geometry, where the magnetic field **B** and QD growth axis **z** enclosed an angle of $\theta = 15^\circ$, in order to allow for the electron spin-flip scattering [13]. The circular polarization of light is denoted by $\sigma^{\pm}$,

*Corresponding author: joerg.debus@tu-dortmund.de

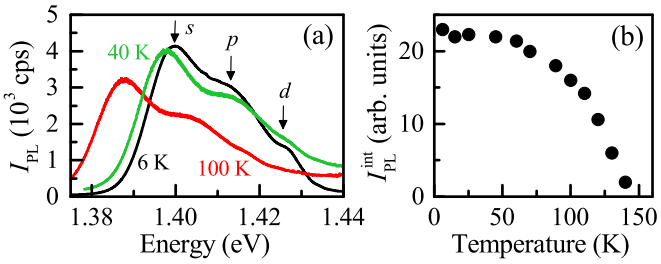

FIG. 1. (a) PL spectra of the singly charged (In,Ga)As/GaAs QDs for different temperatures; $B = 6$ T, $\theta = 90°$. (b) Temperature dependence of the integrated PL intensity.

where the signs $\pm$ are determined by the sign of the photon angular momentum projection on the optical z axis.

The QD photoluminescence (PL), excited with $E_{\mathrm{exc}} = 1.460$ eV laser light, is presented in Fig. 1(a) for 6, 40, and 100 K. At 6 K, the QD emission due to ground state trion recombination is centered at about 1.399 eV, emission from the first (second) excited state is seen around 1.412 eV (1.425 eV); they are marked by arrows in Fig. 1(a). The QD PL at 40 K (100 K) is redshifted in energy by approximately 2 meV (11 meV). It is worthwhile to note that the wetting layer resonance was found at about 1.480 eV at 1.8 K [15]. The PL intensity integrated over the s-, p-, and d-shell spectral range does not vary significantly with increasing temperature up to about 60 K, as depicted in Fig. 1(b) [16]. For larger temperatures, the QD emission weakens gradually and vanishes at about 145 K ($\approx$12 meV), which is associated with the thermally induced dissociation of the trions due to carrier escape from the QDs [17].

The Stokes and anti-Stokes electron (e) spin-flip lines are shown in dependence on the sample temperature in Fig. 2(a), for resonantly exciting the high-energy flank of the s-shell PL at 6 T in Voigt geometry. Below 10 K the intensities of the SFRS lines are relatively weak (300 cps), while the peak intensities significantly rise up to about 1800 cps at 28 K. For $T \geqslant 30$ K, the e-SFRS line intensities decrease. The ratios between the Stokes and anti-Stokes intensities do not vary, e.g., the Stokes scattering signal in the (σ^+,σ^+) copolarized configuration is approximately 10% more intense than the anti-Stokes line for (σ^-,σ^-) throughout the temperature range measured. Moreover, the absolute Raman shift remains at about (185 ± 10) μeV with increasing temperature.

The polarization properties of the electron-SFRS are temperature independent, as is shown in Fig. 2(b) exemplarily for three different temperatures and the copolarized configurations in tilted geometry. At all three temperatures the ratios of the e-SFRS intensities for the polarization configurations (σ^+,σ^+):(σ^+,σ^-):(σ^-,σ^+):(σ^-,σ^-) are approximately given by 1 : 0.19 : 0.27 : 0.19, for the Stokes regime, and 0.19 : 0.30 : 0.16 : 1, for the anti-Stokes regime. Additionally, the maximum of the resonance profile does not demonstrate a temperature-dependent energy shift; it remains approximately at the high-energy flank of the s-shell transition [14], as illustrated in Fig. 2(c). The temperature independences of the Raman shift, Stokes-to-anti-Stokes scattering ratio, resonance-profile spectral position, and optical selection rules indicate that the SFRS of the resident electron occupying the s shell

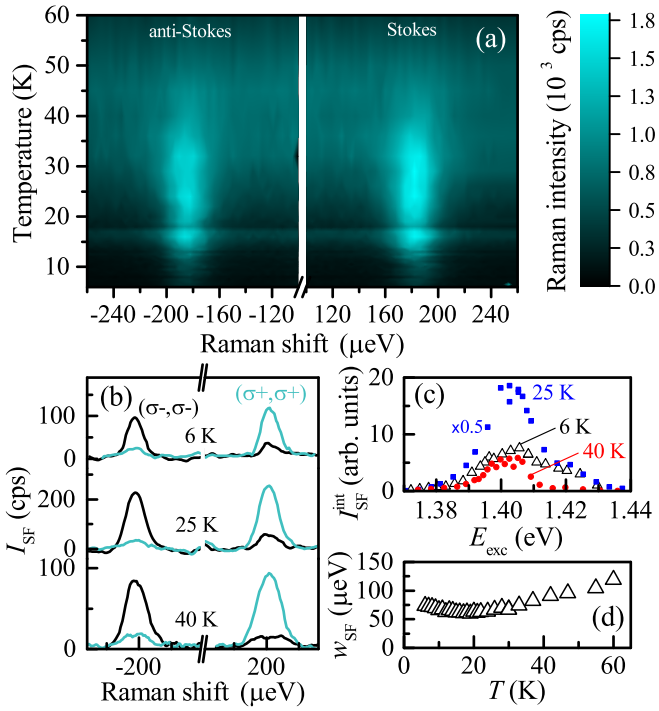

FIG. 2. (a) Image plot of the temperature-dependent intensity of the resident electron-SFRS, for the Stokes and anti-Stokes regime; $B = 6$ T, $\theta = 90°$, $E_{\mathrm{exc}} = 1.406$ eV. The laser line area from -100 to $+100$ μeV is excluded from the image plot. (b) Co-circular polarization properties of the Stokes and anti-Stokes e-SFRS line at $T = 6$, 25, and 40 K and $B = 6$ T; $\theta = 15°$. The background was subtracted from the spectra using similar parameters for the Stokes and anti-Stokes regime. (c) Resonance profiles of the e-SFRS at $B = 6$ T and $\theta = 90°$. (d) Temperature dependence of the e-SFRS linewidth; the error does not exceed the symbol size.

is probed and the basic spin-flip scattering mechanism is not altered [18].

As depicted in Fig. 2(d), the width of the e-SFRS line decreases slightly with rising temperature from 6 to about 20 K, and broadens at temperatures of decreasing e-SFRS intensity ($T > 30$ K). In that temperature range the shape of the SFRS line is well described by a Gaussian profile. The change of the e-SFRS linewidth is of particular interest, since it reveals the decline mechanism of the e-SFRS process, as will be discussed later.

The temperature-dependent enhancement of the e-SFRS intensity is presented by the solid squares in Figs. 3(a)–3(d) as function of the excitation energy E_{exc} that is tuned across the different QD shells. The enhancement factor displays the respective intensity normalized to the value measured at 6 K. The e-SFRS efficiency is most enhanced, up to 6 times, with increasing temperature for resonantly exciting the trion in the s shell and the transition range of the s and p shell. For higher excited states, the thermal enhancement is weaker; for d-shell excitation, there is no enhancement at all. The e-SFRS intensity decreases rapidly above about 28 K, independent of E_{exc}. On the contrary, the background (BG) in the SFRS spectra rises up to 40 K, see open circles, reaching values of $\eta_{\mathrm{BG}} \approx 9$ [19]. It shows a significant enhancement for s- and p-shell excitation. Both the Stokes as well as anti-Stokes background intensities

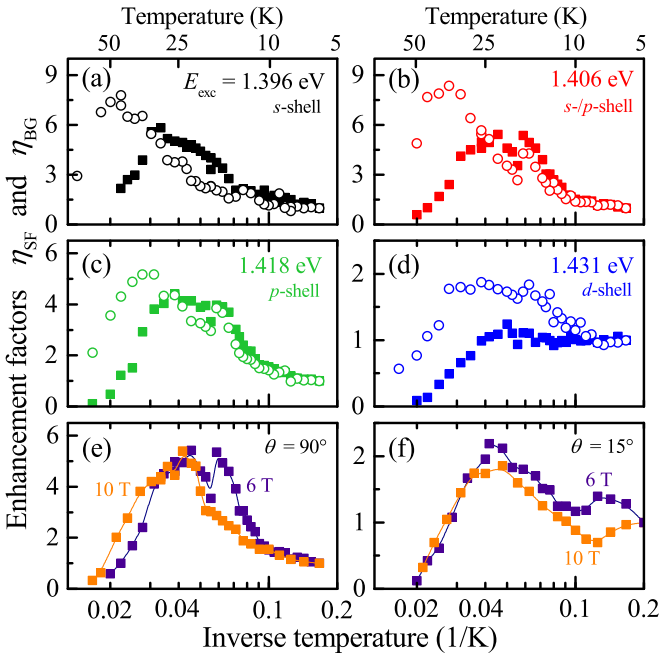

FIG. 3. (a)–(d) Dependence of the enhancement factors of the e-SFRS intensity η_{SF} (solid squares) and SFRS-spectrum background η_{BG} (open circles), on the inverse temperature for different excitation energies; $B = 6$ T, $\theta = 90°$, logarithmic x axis. Note, for $E_{exc} = 1.392$ and 1.399 eV, $\eta_{SF}(1/T)$ is similar to that shown in (a). Temperature dependence of η_{SF} at 6 and 10 T in (e) Voigt geometry and (f) tilted geometry; $E_{exc} = 1.406$ eV. The error does not exceed the symbol size.

demonstrate these dependences. Moreover, they practically coincide with each other for $T \geqslant 10$ K, as one can see in Fig. 2(a). Additionally, both enhancement factors demonstrate a sharp dip at about 18 K, which also manifests itself in the image plot of Fig. 2(a), showing up only for probing the s-/p-shell and p-shell trion.

Figures 3(e) and 3(f) indicate that, on the one hand, in tilted geometry the thermal enhancement of the e-SFRS intensity is considerably smaller than that in Voigt geometry. On the other hand, in a given geometry η_{SF} only weakly responds to the applied magnetic field strength. Moreover, one may claim that the dip in η_{SF} disappears at 10 T in Voigt geometry and, in tilted geometry, it may shift from 18 to 10 (8) K at 6 (10) T. It is worthwhile mentioning that the suppression of the e-SFRS intensity occurs at a temperature, which is several times smaller than the PL quenching temperature.

Let us discuss now the mechanism of the thermal enhancement of the e-SFRS efficiency. The SFRS intensity is generally determined by the product $I_{SF} \propto I_i\, W_{em}\, \tau_j\, W_{SF}\, \tau_j\, W_{abs}$. Here the lifetime τ of the trion in a specific state with total angular momentum j is expected to shorten with increasing temperature due to additional scattering. The intensity of the incident light I_i is kept constant and the absorption W_{abs} and emission W_{em} probabilities, depending on the trion resonance energies, do not change significantly for $T < 40$ K. Of main relevance is therefore the scattering probability W_{SF}, which is governed by Pauli's exclusion principle and the electric-dipole selection rules.

In a slightly tilted geometry the electron-spin basis eigenstates $|s_z = +1/2\rangle = |\uparrow\rangle$ and $|-1/2\rangle = |\downarrow\rangle$ are mixed; for $B > 0$ and a negative electron g factor, the lowest spin state reads $\alpha|\uparrow\rangle + \beta|\downarrow\rangle$ with the mixing coefficients $\alpha \gg \beta$ [14]. Resonant σ^+ polarized laser light excites the first component of the superposition state to a trion resulting in $\alpha\ |\uparrow\downarrow\Uparrow\rangle + \beta\ |\downarrow\rangle$, where $\Uparrow$ denotes the total angular momentum projection $j_{z,hh} = +3/2$ of the heavy hole (hh). An electron spin-flip can then occur in the second component only, so that the intermediate state reads $\alpha\ |\uparrow\downarrow\Uparrow\rangle + \beta\ |\uparrow\rangle$; finally, the light is scattered back with σ^+ circular polarization and the resident electron is left with pure spin-up orientation.

The coherent spin scattering of the resident electron is primarily mediated by exchange interaction with the photoexcited electron [14,15]. However, the second component of the resident-electron spin state can also be reversed through acoustic phonon scattering [13,20]. While its probability is weak at low temperature, it increases with rising temperature due to the increase in the density of populated acoustic phonon modes. Thus, at elevated temperatures both electron-electron exchange as well as acoustic phonon scattering realize the e-SFRS. Of relevance for the thermal SFRS efficiency enhancement at particularly s-shell excitation may be an acoustic-phonon induced coupling of the energetically lowest singlet s-shell trion with excited trion states [21], such as the triplet or singlet p-shell trions. These states are characterized by nonzero orbital angular momentum; hence, the corresponding mixture of spin and orbital electron states opens further spin-flip scattering channels yielding an enhanced e-SFRS efficiency. The acoustic-phonon supported electron-SFRS modifies neither the Raman shift nor the polarization of the scattered light because of the unchanged $j_{z,hh}$. Due to the spin-orbital state mixing one may expect that, e.g., in the Stokes regime, the (σ^-,σ^-) polarized SFRS line becomes more intense; however, this configuration leads to parallel e-spin orientation, whose formation is restricted by Pauli's exclusion principle. Moreover, for exciting higher lying states of, e.g., the d-shell trion, the scattering efficiency weakens significantly, since the spin scattering becomes strongly off-resonant and the lifetime of these excited states is short.

Our explanation is further underlined by the increase in the scattering background, which we attribute mainly to acoustic phonon scattering, while we propose that resonant PL gives a negligible contribution to the SFRS spectra measured. The similar Stokes and anti-Stokes BG intensities resemble the acoustic phonon sidebands of zero-phonon lines in QDs. Their spectral contribution increases approximately by one order of magnitude from 10 to 50 K [4,22], which agrees with our enhancement factors. Due to the broken k-vector conservation in QDs, the scattering BG is broad and is not restricted to specific acoustic phonon frequencies [20]. One may argue in comparison to quantum wells that the QD in-plane confinement results in a shift of the acoustic-phonon scattering maximum to the laser line. And, if resonantly excited PL formed the BG, it would show a temperature dependence similar to that of the below-wetting-layer excited PL, which is however not the case.

The e-SFRS line broadening, for $T > 30$ K, indicates a process counteracting the enhancement of the coherent SFRS through the thermal acoustic phonons. We ascribe the

broadening and intensity reduction of the e-SFRS line to (i) an acceleration of the transverse electron spin relaxation and, in particular, (ii) to pure trion dephasing caused by charge fluctuations in the QD environment and also acoustic phonon interaction [23–25]. With rising sample temperature, we thus assign the constructive and destructive effects on the electron-SFRS to the acoustic phonons. One can expect that the pure dephasing is only weakly affected by the magnetic field strength and orientation, as is outlined by the similar deactivation temperatures of the e-SFRS process. The decrease in the e-SFRS intensity begins at temperatures, at which also the linewidth starts to broaden, while the scattering BG becomes still more intense. The deactivation of the e-SFRS process occurs at temperatures, where the trion is far from being dissociated, while the reduction in the BG intensity can be attributed to the energy shift of the trion resonance with increasing temperature. On the contrary, the slight narrowing of the linewidth may hint at a stabilization of the trion coherence.

For the sake of completeness, we like to discuss temperature-dependent phenomena in self-assembled QDs that can be excluded as relevant mechanisms. (i) A thermally activated transfer of electrons between differently strong confining, spatially adjacent QDs [26] may cause the increase in the spin-flip scattering efficiency. This interdot coupling or tunneling would increase the number of single-charged dots, in which the e-SFRS could occur, and could also explain the weakly increased e-SFRS intensity in the tilted geometry due to the magnetic confinement leading to an enhanced electron localization. However, this model requires a quite rare configuration of resident carrier occupations in the QDs, namely QDs with two and without resident electrons, in order to achieve a positively balanced number of singly charged dots. (ii) A thermal activation of trapped or wetting-layer electrons [27] that relax into undoped QDs would enhance the e-SFRS scattering efficiency. Nevertheless, this thermal activation should not depend on the magnetic field geometry, and, for singly charged QDs, it requires the presence of a large number of undoped QDs probed at low and high excitation energies. This can also be neglected for the QD ensembles studied [28]. (iii) Electron-nuclear hyperfine interaction leading to an enhanced spin-flip scattering efficiency can be ruled out already for temperatures above 6 K, as shown in Ref. [15]. In this case one would also expect a shift in the e-SFRS line position due to a temperature-dependent change in the Overhauser field [29].

Finally, the focus shall be drawn on the sharp drop in the e-SFRS and BG intensities at 18 K observed for excitation in the *s*-/*p*- and *p*-shell ranges. This temperature corresponds to 1.6 meV, which is several times smaller than the lateral confinement energy of the QDs in the conduction and valence band. One may attribute the intensity drop to a *p*-orbital splitting in the conduction band resulting from the noncircular shape of the QDs, so that a loss channel for the electron spin-flip efficiency is opened. Since also the scattering BG demonstrates this intensity dip, it is, however, also possible that the trion coherence is disturbed by acoustic phonons with energies of 1–2 meV, whose wave functions fit into the QDs having an average diameter of 20–30 nm, thus leading to a maximum scattering matrix element. The drop occurs at small temperatures for a strong in-plane magnetic confinement, as depicted in Fig. 3(f), which on the other hand favors the explanation of the electron-SFRS damping due to a *p*-orbital splitting.

In conclusion, the efficiency of the coherent spin-flip Raman scattering of the resident electron is significantly increased with rising sample temperature, for resonant trion excitation in (In,Ga)As/GaAs QDs. Thermal acoustic phonons enhance the electron spin-flip scattering efficiency, while pure trion dephasing may suppress the electron-SFRS at about 50 K. Our results demonstrate that thermal phonons do not disturb the coherent SFRS process primarily based on electron exchange interaction, thus emphasizing that it is worth to pursue coherent spin physics in III-V semiconductor nanostructures above 10 K aiming for spin applications at liquid-nitrogen temperature.

We acknowledge financial support by the Deutsche Forschungsgemeinschaft in the frame of the ICRC TRR 160 (Projects No. B2 and Z1), the BMBF within the Q.com-H consortium (Projects No. 16KIS0104K and No. 16KIS0109), and the Russian Science Foundation (Project No. 14-42-00015).

[1] Edited by A. Tartakovskii, *Quantum Dots: Optics, Electron Transport and Future Applications* (Cambridge University Press, Cambridge, 2012).

[2] A. Ebbens, D. N. Krizhanovskii, A. I. Tartakovskii, F. Pulizzi, T. Wright, A. V. Savelyev, M. S. Skolnick, and M. Hopkinson, Optical orientation and control of spin memory in individual InGaAs quantum dots, Phys. Rev. B **72**, 073307 (2005).

[3] E. Poem, O. Kenneth, Y. Kodriano, Y. Benny, S. Khatsevich, J. E. Avron, and D. Gershoni, Optically Induced Rotation of an Exciton Spin in a Semiconductor Quantum Dot, Phys. Rev. Lett. **107**, 087401 (2011).

[4] L. Besombes, K. Kheng, L. Marsal, and H. Mariette, Acoustic phonon broadening mechanism in single quantum dot emission, Phys. Rev. B **63**, 155307 (2001).

[5] S. Adachi, N. Yatsu, R. Kaji, S. Muto, and H. Sasakura, Decoherence of exciton complexes in single InAlAs quantum dots measured by Fourier spectroscopy, Appl. Phys. Lett. **91**, 161910 (2007).

[6] A. Greilich, M. Wiemann, F. G. G. Hernandez, D. R. Yakovlev, I. A. Yugova, M. Bayer, A. Shabaev, Al. L. Efros, D. Reuter, and A. D. Wieck, Robust manipulation of electron spin coherence in an ensemble of singly charged quantum dots, Phys. Rev. B **75**, 233301 (2007).

[7] F. G. G. Hernandez, A. Greilich, F. Brito, M. Wiemann, D. R. Yakovlev, D. Reuter, A. D. Wieck, and M. Bayer, Temperature-induced spin-coherence dissipation in quantum dots, Phys. Rev. B **78**, 041303(R) (2008).

[8] P. C. Maurer, G. Kucsko, C. Latta, L. Jiang, N. Y. Yao, S. D. Bennett, F. Pastawski, D. Hunger, N. Chisholm, M. Markham, D. J. Twitchen, J. I. Cirac, and M. D. Lukin, Room-temperature quantum bit memory exceeding one second, Science **336**, 1283 (2012).

[9] M. Widmann, S.-Y. Lee, T. Rendler, N. T. Son, H. Fedder, S. Paik, L.-P. Yang, N. Zhao, S. Yang, I. Booker, A. Denisenko, M. Jamali, S. A. Momenzadeh, I. Gerhardt, T. Ohshima, A. Gali, E. Janzén, and J. Wrachtrup, Coherent control of single spins in silicon carbide at room temperature, Nat. Mater. **14**, 164 (2015).

[10] H. Gotoh, H. Sanada, H. Yamaguchi, and T. Sogawa, Modifying exciton optical properties in quantum dots with coherent phonons induced by ultrafast optical pulses, Appl. Phys. Lett. **103**, 112104 (2013).

[11] A. M. Barth, S. Lüker, A. Vagov, D. E. Reiter, T. Kuhn, and V. M. Axt, Fast and selective phonon-assisted state preparation of a quantum dot by adiabatic undressing, Phys. Rev. B **94**, 045306 (2016).

[12] J. Debus, T. S. Shamirzaev, D. Dunker, V. F. Sapega, E. L. Ivchenko, D. R. Yakovlev, A. I. Toropov, and M. Bayer, Spin-flip Raman scattering of the Γ-X mixed exciton in indirect band gap (In, Al)As/AlAs quantum dots, Phys. Rev. B **90**, 125431 (2014).

[13] J. Debus, D. Dunker, V. F. Sapega, D. R. Yakovlev, G. Karczewski, T. Wojtowicz, J. Kossut, and M. Bayer, Spin-flip Raman scattering of the neutral and charged excitons confined in a CdTe/(Cd, Mg)Te quantum well, Phys. Rev. B **87**, 205316 (2013).

[14] J. Debus, V. F. Sapega, D. Dunker, D. R. Yakovlev, D. Reuter, A. D. Wieck, and M. Bayer, Spin-flip Raman scattering of the resident electron in singly charged (In, Ga)As/GaAs quantum dot ensembles, Phys. Rev. B **90**, 235404 (2014).

[15] J. Debus, D. Kudlacik, V. F. Sapega, D. Dunker, P. Bohn, F. Paßmann, D. Braukmann, J. Rautert, D. R. Yakovlev, D. Reuter, A. D. Wieck, and M. Bayer, Nuclear spin polarization in the electron spin-flip Raman scattering of singly charged (In, Ga)As/GaAs quantum dots, Phys. Rev. B **92**, 195421 (2015).

[16] The PL intensities integrated separately over the s, p, or d shell show similar behavior.

[17] R. Oulton, A. I. Tartakovskii, A. Ebbens, J. Cahill, J. J. Finley, D. J. Mowbray, M. S. Skolnick, and M. Hopkinson, Temperature-induced carrier escape processes studied in absorption of individual In_xGa_{1-x} As quantum dots, Phys. Rev. B **69**, 155323 (2004).

[18] The Raman shift, see Fig. 2(a), may not deviate with temperature, since QDs with a specific band-gap energy, which mainly contributes to the electron g factor, are excited by a fixed laser energy.

[19] The background intensities are evaluated from baseline fits of the Raman spectra between the lower and upper limits of 110 and 260 μeV, respectively.

[20] A. A. Sirenko, V. I. Belitsky, T. Ruf, M. Cardona, A. I. Ekimov, and C. Trallero-Giner, Spin-flip and acoustic-phonon Raman scattering in CdS nanocrystals, Spin-flip and acoustic-phonon Raman scattering in CdS nanocrystals, Phys. Rev. B **58**, 2077 (1998).

[21] E. B. Flagg, J. W. Robertson, S. Founta, W. Ma, M. Xiao, G. J. Salamo, and C.-K. Shih, Direct Evidence of Interlevel Exciton Transitions Mediated by Single Phonons in a Semiconductor Quantum Dot Using Resonance Fluorescence Spectroscopy, Phys. Rev. Lett. **102**, 097402 (2009).

[22] I. Favero, G. Cassabois, R. Ferreira, D. Darson, C. Voisin, J. Tignon, C. Delalande, G. Bastard, Ph. Roussignol, and J. M. Gérard, Acoustic phonon sidebands in the emission line of single InAs/GaAs quantum dots, Phys. Rev. B **68**, 233301 (2003).

[23] P. Borri, W. Langbein, U. Woggon, V. Stavarache, D. Reuter, and A. D. Wieck, Exciton dephasing via phonon interactions in InAs quantum dots: Dependence on quantum confinement, Phys. Rev. B **71**, 115328 (2005).

[24] I. Favero, A. Berthelot, G. Cassabois, C. Voisin, C. Delalande, Ph. Roussignol, R. Ferreira, and J. M. Gérard, Temperature dependence of the zero-phonon linewidth in quantum dots: An effect of the fluctuating environment, Phys. Rev. B **75**, 073308 (2007).

[25] A. Berthelot, I. Favero, G. Cassabois, C. Voisin, C. Delalande, Ph. Roussignol, R. Ferreira, and J. M. Gérard, Unconventional motional narrowing in the optical spectrum of a semiconductor quantum dot, Nat. Phys. **2**, 759 (2006).

[26] C. Hermannstädter, N. A. Jahan, J.-H. Huh, H. Sasakura, K. Akahane, M. Sasaki, and I. Suemune, Inter-dot coupling and excitation transfer mechanisms of telecommunication band InAs quantum dots at elevated temperatures, New J. Phys. **14**, 023037 (2012).

[27] A. Musial, G. Sek, A. Marynski, P. Podemski, J. Misiewicz, A. Löffler, S. Höfling, S. Reitzenstein, J. P. Reithmaier, and A. Forchel, Temperature dependence of photoluminescence from epitaxial InGaAs/GaAs quantum dots with high lateral aspect ratio, Acta Phys. Pol. A **120**, 883 (2011).

[28] This possibility has been simulated by additional unpolarized wetting-layer excitation leading only to a slight increase (factor 1.5) in the e-SFRS intensity at 6 K. Note, for the wetting-layer excitation both electrons and holes are excited; thus, it could not fully simulate a thermal activation of trapped electrons.

[29] B. Urbaszek, P.-F. Braun, T. Amand, O. Krebs, T. Belhadj, A. Lemaítre, P. Voisin, and X. Marie, Efficient dynamical nuclear polarization in quantum dots: Temperature dependence, Phys. Rev. B **76**, 201301(R) (2007).